Peptide Models Provide Evidence for Significant Structure in the Denatured State of a Rapidly Folding Protein: The Villin Headpiece Subdomain†

Yuefeng Tang,§ Daniel J. Rigotti,‡ Robert Fairman,‡ and Daniel P. Raleigh*,§,#

Department of Chemistry, State University of New York at Stony Brook, Stony Brook, New York 11794-3400, Graduate Program in Biochemistry and Structural Biology, State University of New York at Stony Brook, Stony Brook, New York 11794, and Department of Molecular, Cell and Developmental Biology, Haverford College, Haverford, Pennsylvania 19041

Received September 12, 2003; Revised Manuscript Received January 10, 2004

ABSTRACT: The villin headpiece subdomain is a cooperatively folded 36-residue, three-α-helix protein. The domain is one of the smallest naturally occurring sequences which has been shown to fold. Recent experimental studies have shown that it folds on the 10-μs time scale. Its small size, simple topology, and very rapid folding have made it an attractive target for computational studies of protein folding. We present temperature-dependent NMR studies that provide evidence for significant structure in the denatured state of the headpiece subdomain. A set of peptide fragments derived from the headpiece were also characterized in order to determine if there is a significant tendency to form a locally stabilized structure in the denatured state. Peptides corresponding to each of the three isolated helices and to the connection between the first and second helices were largely unstructured. A longer peptide fragment which contains the first and second helices shows considerable structure, as judged by NMR and CD. Concentration-dependent CD measurements and analytical ultracentrifugation experiments indicate that the structure is not due to self-association. NMR studies indicate that the structure is stabilized by tertiary interactions involving phenylalanines and Val 50. A peptide in which two of the three phenylalanines are changed to leucine is considerably less structured, confirming the importance of the phenylalanines. This work indicates that there is significant structure in the denatured state of this rapidly folding protein.

Characterization of the denatured state is required for a complete description of protein folding and protein stability (*1*, *2*). Of most relevance to folding are the properties of the denatured state ensemble, which is in equilibrium with the folded state under native conditions. Unfortunately, this state is difficult to study because the denatured state survives only transiently during refolding experiments and is only weakly populated at equilibrium. There have been many reports of studies of unfolded proteins in strongly denaturing condition. In contrast, there are very few studies of the properties of the denatured state populated under native conditions. In most cases, indirect approaches have to be used to characterize this state. One strategy is to characterize peptide fragments corresponding to the elements of secondary structure in the protein (*3*). Although short peptide fragments lack any long-range tertiary interactions which may stabilize denatured state structure in the full-length protein, they do provide a means of identifying locally stabilized structure. The inference is that any structure observed in small peptide fragments can form in the denatured state. Here we use this approach to characterize the tendency to form locally stabilized structure in the denatured state of the villin headpiece helical subdomain (HP36).[1] These experiments are supplemented by temperature-dependent NMR studies of intact HP36. HP36, at 36 residues, is one of the smallest naturally occurring sequences which has been shown to fold cooperatively (*4*−*6*). Recently, we and Eaton and colleagues have independently demonstrated that HP36 folds on the microsecond time scale (*7*, *8*). A ribbon diagram of the protein is shown in Figure 1. The domain is stabilized by a well-packed hydrophobic core made up of Phe 47, Phe 51, Phe 58, and Val 50 as well as several other residues (*5*, *6*). These three phenylalanines play an important role in stabilizing the structure and are depicted in Figure 1.

Its small size, simple three-helix topology, and rapid folding have made it a popular target for computational studies of protein folding. These studies have typically attempted to fold HP36 starting from an extended structure. In many cases, a very rapid collapse to a much more compact

† This research was supported by NIH Grant GM 54233 to D.P.R.

* To whom correspondence should be addressed. Telephone: (631) 632-9547. Fax: (631) 632-7960. E-mail: draleigh@notes.cc.sunysb.edu.

§ Department of Chemistry, State University of New York at Stony Brook

Graduate Program in Biochemistry and Structural Biology, State University of New York at Stony Brook.

‡ Haverford College.

[1] Abbreviations: CD, circular dichroism; Fmoc, 9-fluorenylmethyloxycarbonyl; HP36, the helical subdomain of the villin headpiece (the peptide corresponds to residues 42−75 of the villin headpiece with an additional Met at the N-terminus; the N-terminal Met is denoted M41); HP−H1, a peptide corresponding to residues M41−M53 of HP36; HP−H2, a peptide corresponding to residues G52−L61 of HP36; HP−H3, a peptide corresponding to residues P62−L75 of HP36; HP−H1/2, a peptide corresponding to residues M41−L61 of HP36; HP−H4, a peptide corresponding to residues D46−S56 of HP36; F47L,F51L,-HP−H1/2, variant of HP−H1/2 in which F47 and F51 are changed to L; HPLC, high-pressure liquid chromatography; TFA, trifluoroacetic acid; DQF-COSY, double-quantum-filtered correlated spectroscopy; TOCSY, total correlation spectroscopy; ROESY, rotating frame nuclear overhauser spectroscopy.

10.1021/bi035652p CCC: $27.50
Published on Web 02/27/2004

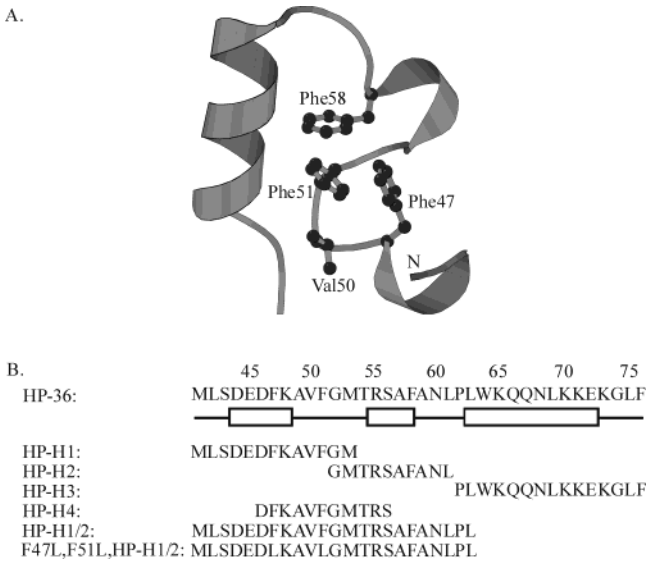

FIGURE 1: (A) Ribbon diagram of the villin headpiece subdomain (HP36), created with the program Molscript (*32*) (PDB code 1VII). The location of the three phenylalanines which contribute to the hydrophobic core is shown, as is the position of the N-terminus. (B) Primary sequence and secondary structure of HP-36 and of the peptide fragments studied in this work. The secondary structure of HP-36 is denoted by the diagram below the sequence. α-Helices are represented as rectangles. The numbering system corresponds to that use for the full-length villin headpiece. The helical subdomain starts at residue L42. However, all of the published experiments with this domain have made use of a construct which contains an initial Met. This residue is designated M41. The N-terminal helix runs from D44 to K48, the central helix from R55 to F58, and the C-terminal helix from L63 to E72. All of the synthetic peptides have an amidated C-terminus. HP−H2 and HP−H3 have acetylated N-termini, while HP−H1 and HP−H1/2 have free N-termini.

state is observed, followed by a slower but still rapid transition to a more native-like state (*9*−*21*). In principle, these studies could provide information about the denatured state. However, the thrust of the work to date has been to fold HP36. Distributed computing methods have also recently been used in an attempt to generate models of the denatured state ensemble of HP36 (*17*). There is very little experimental data available to compare with these computational studies. Thus, it is not clear if the very rapid collapse observed in the same simulations represents a transition along the folding pathway or instead represents a rearrangement from the initial extended conformation used in these studies. Given its rapid folding and choice as a popular test system for simulation, it is clearly desirable to characterize the conformational propensities of the denatured state of HP36 in as much detail as possible. Local structure plays a central role in the diffusion collision model of the folding of all helical proteins (*9*, *22*), so it is of particular interest to examine the propensity to form local structure. Initial amide H/D exchange experiments provided some evidence for nonrandom structure in the denatured state of HP36. In particular, McKnight and co-workers observed that several amides exchanged significantly slower than predicted by global unfolding using the known value of ΔG° (*4*). This suggests the presence of some denatured state structure which provides additional protection to these sites.

In this work, six peptide fragments derived from HP36 were characterized. Five make up a set of overlapping fragments, while the sixth is a variant including substitution of two phenylalanines. HP−H1, HP−H2, and HP−H3 correspond to each of the three isolated α-helices starting from the N-terminus. HP−H4 encompasses the connection between helix-1 and helix-2. The fifth peptide is a longer construct which includes the first and second helices. This peptide is denoted HP−H1/2. The sixth peptide is a variant of HP−H1/2 in which two phenylalanines were changed to leucine. The sequence of HP36 and the peptide fragments are shown in Figure 1B. The numbering system used here is chosen for consistency with earlier publications on the intact helical subdomain (*4*, *5*). The helical subdomain consists of residues 42−76 of the villin headpiece; however, all published studies have made use of a construct which includes an additional N-terminal methionine. This residue is designated Met 41, and it is the first residue in HP36. The C-terminal residue is Phe 76. This notation is also consistent with that used by McKnight and co-workers in their structural studies of HP36.

MATERIALS AND METHODS

Peptide Synthesis and Purification. Six peptide fragments, derived from the sequence of HP36, were synthesized. HP−H1 (M41−M53) corresponds to the N-terminal α-helix of HP36. HP−H2 (G52−L61) was prepared to include the second helix. HP−H3 (P62−L75) contains the C-terminal helix. HP−H4 is made up of residues 46−56 and includes the connection between helix-1 and helix-2. A longer peptide fragment HP−H1/2 (M41−L61) includes the N-terminal helix and the second helix. A variant of this peptide was prepared in which Phe 47 and Phe 51 were both changed to Leu. This peptide is denoted F47L,F51L,HP−H1/2. All peptides were prepared on a 0.25 mmol scale by standard solid-phase Fmoc chemistry using an Applied Biosystems 433A automated peptide synthesizer. 1-Methyl-2-pyrrolidone (NMP) was used as the major solvent in synthesis. Standard reaction cycles were used. The first residue linked to the resin and amino acids containing β-branched side chains were doubly coupled. PAL-PEG-PS resin was used, giving amidated C-termini upon cleavage from the resin. The cleavage cocktail was a 91% trifluoroacetic acid (TFA)/3% anisole/3% thioanisole/3% ethanedithiol mixture. HP−H1, HP−H1/2, and F47L,F51L,HP−H1/2 have free N-termini, while HP−H2, HP−H3, and HP−H4 are N-terminal acetylated. After cleavage, all peptides were purified by high-pressure liquid chromatography (HPLC) on a semipreparative C18 reverse-phase column (Vydac) using a water/acetonitrile gradient containing 0.1% TFA. All peptides were greater than 95% pure after purification as judged by analytical HPLC. The identity of each peptide was confirmed by matrix-assisted laser desorption and ionization time-of-flight mass spectrometry (MALDI-TOF). The expected and observed molecular weights were as follows: HP−H1, expected 1489.7, observed 1490.4; HP−H2, expected 1109.2, observed 1109.4; HP−H3 expected 1750.1, observed 1751.7; HP−H4, expected 1300.4, observed 1298.9; HP−H1/2, expected 2350.7, observed 2350.1; F47L,F51L,HP−H1/2, expected 2282.1, observed 2283.1.

Circular Dichroism (CD) Spectroscopy. All CD experiments were performed using Aviv 62A DS and 202SF circular dichroism spectrophotometers. Samples were buffered using 10 mM sodium acetate and 150 mM sodium chloride at pH 5.0. These conditions were chosen to mimic

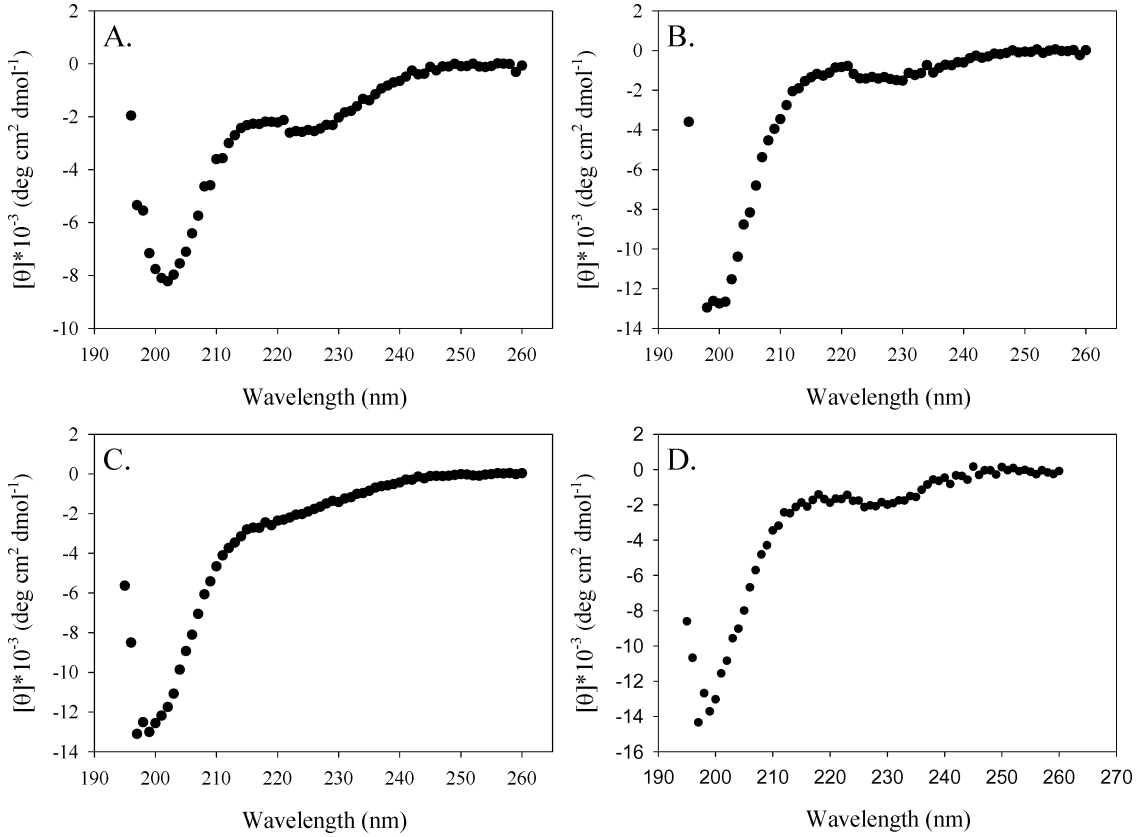

FIGURE 2: Far-UV CD spectra of (A) HP−H1, (B) HP−H2, (C) HP−H3, and (D) HP−H4. All spectra were obtained at 25 °C, 150 mM sodium chloride, 10 mM sodium acetate buffer at pH 5.0.

earlier studies on full-length HP36. All far-UV wavelength scans were performed using a 1 mm quartz cuvette with five repeats and an averaging time of 1 s at each wavelength. Spectra were collected from 195 to 260 nm. The protein concentrations were determined from absorbance measurements using the method described by Pace and co-workers (*23*). The absorbance was measured at either 280 nm (for HP−H3) or 257 nm (for HP−H1, HP−H2, HP−H4, HP−H1/2 and F47L,F51L,HP−H1/2) in 6 M guanidine hydrochloride, 20 mM sodium phosphate pH 6.5, using calculated extinction coefficients of 394 M^{-1} cm^{-1} for HP−H1, 197 M^{-1} cm^{-1} for HP−H2, 5690 M^{-1} cm^{-1} for HP−H3, 394 M^{-1} cm^{-1} for HP−H4, 591 M^{-1} cm^{-1} for HP−H1/2, and 197 M^{-1} cm^{-1} for F47L,F51L,HP−H1/2, respectively. pH-titration experiments were performed in a 1 cm stirred quartz cuvette at 25 °C. The signal at 222 nm was monitored and averaged for 60 s. pH values were changed by adding ∼0.2−1 μL of HCl or NaOH to the sample. Peptide concentrations were 134 μM for HP−H1, 60 μM for HP−H3, and 30 μM for HP−H1/2. The concentration dependences of the CD signal of HP−H1/2 and of F47L,F51L,HP−H1/2 were examined at pH 5.0.

Nuclear Magnetic Resonance (NMR) Spectroscopy. One- and two-dimensional proton NMR spectra were recorded on Varian Instruments Inova 500 and 600 MHz spectrometers. One-dimensional spectra were collected using a standard water presaturation sequence. Two-dimensional spectra including DQF-COSY (double-quantum-filtered correlated spectroscopy), TOCSY (total correlation spectroscopy), and ROESY (rotating frame nuclear Overhauser spectroscopy) spectra were recorded for HP−H1, HP−H2, HP−H3, and HP−H4 at 25 °C. The spectral width in both dimensions was 8000 Hz. Chemical shifts were referenced to sodium 3-trimethylsilyl-2,2,3,3-d_4 propionate (TSP) at 0.0 ppm. The mixing time was 75 ms for the TOCSY experiments and 250 ms for the ROESY experiment. Chemical shift assignments were made using standard procedures. HP−H2, HP−H3, and HP−H4 were each at a concentration of 2 mM in 90% H_2O/10% D_2O, 10 mM sodium acetate, and 150 mM sodium chloride at pH 5.0. Samples of HP−H1 were prepared in the same buffer at 800 μM and pH 5.5. The deviation of C_α proton chemical shifts from random coil values was calculated using random coil chemical shifts taken from Wishart et al. (*24*). The larger peptide HP−H1/2 shows some association above a concentration of 350 μM. TOCSY and ROESY spectra were acquired in 99.9% D_2O buffer for a 400 μM sample at pD 5.5 using mixing times of 75 ms for TOCSY and 250 ms for ROESY. One-dimensional spectral were recorded at 150 and 400 μM. The line widths were larger for the 400 μM sample but the chemical shifts were unchanged. A one-dimensional NOE difference spectrum was collected on the same HP−H1/2 peptide solution.

Analytical Ultracentrifugation. Protein samples were prepared in 10 mM sodium acetate pH 5.0 and 150 mM NaCl. Samples of HP−H1/2 were loaded at concentrations of 350 and 150 μM each into six-channel, 12 mm path length, charcoal-filled Epon cells. Sedimentation equilibrium experiments were carried out at both 5 and 25°C with a Beckman Optima XL-A analytical ultracentrifuge equipped with an An60 Ti rotor using rotor speeds of 30 000, 40 000, and 50 000 rpm. Temperature-corrected partial specific volumes and solution density were calculated using the Sednterp program (*25*). Data analysis was carried out using Win Nonlin (v. 1.06) obtained from the Analytical Ultracentrifu-

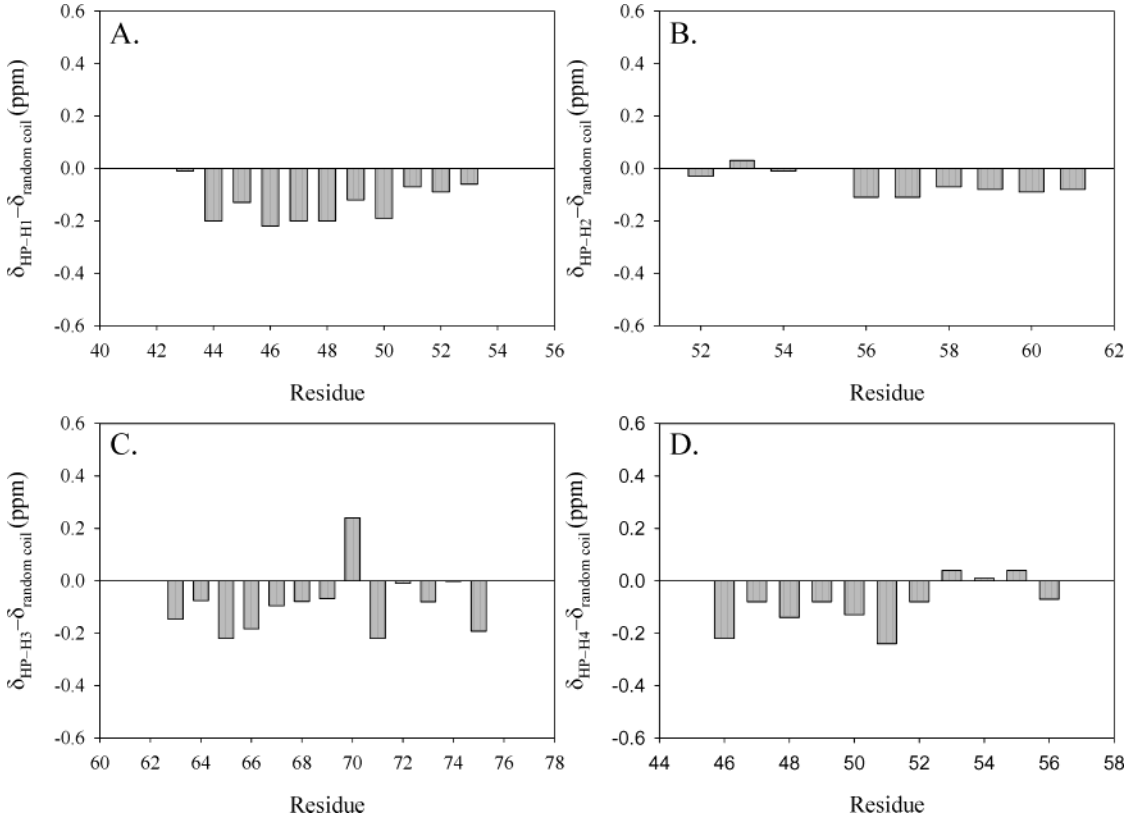

FIGURE 3: Deviations of the C_α proton chemical shift from random coil values. (A) HP−H1, (B) HP−H2, (C) HP−H3, and (D) HP−H4. Data were collect at 25 °C for all peptides in 150 mM sodium chloride and 10 mM sodium acetate. The pH was 5.5 for HP−H1 and 5.0 for the other peptides.

gation Facility website, University of Connecticut, Storrs, CT.

RESULTS

Design of Peptide Fragments. A series of overlapping peptides were designed corresponding to different secondary structure elements of HP36. Their location in the native state of HP36 is shown in Figure 1A, and the sequences are listed in Figure 1B. Three peptides, HP−H1 (residues M41−M53), HP−H2 (residues G52−L61), and HP−H3 (residues P62−L75), were prepared that correspond to the helical segments of HP36 starting from the N-terminus. The peptides include the sequence of the helices and several flanking residues. In the native state the first helix runs from D44 to K48, the second from R55 to F58, and the third from L63 to E72. Helix-1 and helix-2 are connected by a region in which the polypeptide chain undergoes a sharp reversal of direction, residues 49−53. This segment includes one residue, G52, with a positive ϕ angle. The fourth peptide, denoted HP−H4, is made up of residues 46−56 and includes this region. It also contains two of the three phenylalanines that pack in the hydrophobic core of the native state as well as Val 50. A longer peptide, HP−H1/2 (residues M41−L61), corresponds to the region made up of the N-terminal and the central α-helix. This region of the chain contains the cluster of three phenlyalanines which have been shown to be important for the stability of HP36 (*26*). Several other residues which contribute to the hydrophobic core, including Val 50, are found in this region. All peptide fragments are amidated at their C-terminius. HP−H1 and HP−H1/2 have a free N-terminus, while HP−H2, HP−H3, and HP−H4 have acetylated N-termini.

Individual Elements of Secondary Structure Do Not Form in Isolation. The far-UV CD spectra of HP−H1, HP−H2, HP−H3, and HP−H4 in acetate buffer at pH 5.0 are shown in Figure 2. On the basis of their CD spectra, these peptides are largely unstructured in solution. The mean residue ellipticity at 222 nm is −2600 for HP−H1, −1200 for HP−H2, −2200 for HP−H3, and −1700 for HP−H4. HP−H1, HP−H2, and HP−H4 do not contain Trp or Tyr; thus, the concentrations of these peptides were determined using phenylalanine absorbance. This is likely less precise than Trp absorbance, so the values of θ_{222} should be regarded as estimates. However, the key point is that the intensity in the region near 222 nm is very weak, and the shape of the spectra is also consistent with a lack of helical structure. The small values of θ_{222} could result from a small tendency to form structure, or they could simply represent the ellipticity of the particular sequence in the denatured state. The addition of 6 M guanidine hydrochloride decreases the intensity at 222 nm, suggesting that the shoulder at 222 nm could arise from real structure which is perturbed by denaturant. The fraction of helix can be estimated using relations given by Baldwin and co-workers or by using the value of θ_{222} in 6 M GuHCl to represent the coil state (*27*). Using the method of Baldwin, the apparent helical content is estimated as 7% for HP−H1, 3% for HP−H2, and 6% for HP−H3. If the spectra in 6 M GuHCl are taken to represent the coil state, similar values are obtained: 7% for HP−H1, 2% for HP−H2, and 6% for HP−H3. In any case, the key observation is that all three peptides have no significant tendency to fold in isolation. Temperature-dependent CD measurements show that lowering the temperature to 5 °C does not increase the apparent α-helix content. HP−H1 and HP−H3 contain

ionizable residues while HP−H2 does not. Consequently, the tendency to form helical structure at different pH values was tested for HP−H1 and HP−H3. For HP−H1, the apparent helical content is lowest at pH 2. An increase in intensity of θ_{222} (becoming more negative) is observed as the acidic side chains are deprotonated, and a further increase is detected as the pH is raised through the pK_a of the N-terminus and Lys side chains. The increase from pH 2 to pH 6 likely reflects the formation of interactions between the acidic side chains and basic residues. The increase at higher pH is most likely due to deprotonation of the N-terminus. Even at the highest pH, the apparent helical content is still small. For the peptide HP−H3, which corresponds to the C-terminal helix, the pH titration curve shows only minor changes in signal intensity at 222 nm. At pH 2 or pH 10, the apparent helix content is only slightly higher than that in the range of pH 3 to pH 9. HP−H4 contains one acidic residue, namely D46 consequently. The CD spectrum was recorded at low pH to test whether protonating this side chain had any significant effect. The spectrum recorded at pH 2.0 is very similar to that at pH 5.0.

NMR studies were undertaken to characterize the conformation of these fragments in more detail. 2D spectra of all of the peptide fragments were recorded at 25 °C and pH 5.0 for HP−H2, HP−H3, and HP−H4 and at pH 5.5 for HP−H1. They could easily be assigned by standard methods. No medium-range NOEs were observed for any of the peptide fragments, indicating a lack of helix or turn formation. A few NH_i to NH_{i+1} NOEs could be observed for the small peptide fragments; however, NH_i to NH_{i+1} NOEs are often observed for unstructured peptides (*28*). $^3J_{HN,\alpha}$ coupling constants are sensitive to the ϕ-angle and are small in helical regions. All of the residues in HP−H1, HP−H2, and HP−H3 have *J*-coupling constants in the range of 5.3−7.4 Hz, consistent with conformational averaging. $C_\alpha H$ chemical shifts are sensitive to secondary structure and are often used to probe the formation of an α-helix or a β-sheet (*24*). Figure 3 shows plots of the difference between the measured $C_\alpha H$ chemical shifts and random coil values for the four peptides. HP−H4 contains residues which are also found in HP−H1 (D46−M53) and HP−H2 (G52−S56). The $C_\alpha H$ shifts of the overlapping residues are similar in the different peptides. With a few exceptions, almost all of the $C_\alpha H$ resonances are shifted slightly upfield. The shifts are all within 0.25 ppm of random coil values, and most are much less. The fragments which show the largest deviation contain the aromatic residues, and this might contribute. Alternatively, the small shifts could suggest that there might be a small propensity to populate the helical region of the ϕ,ψ map. In any case, the NMR conformational analysis is consistent with the CD studies, showing that all the small peptide fragments are basically unstructured.

A Larger Peptide Made Up of the First Two Helices Contains Significant Structure. The results presented in the previous section clearly demonstrate that the individual helices and the region connecting helix-1 and helix-2 have very little tendency to fold in isolation. The situation is dramatically different when the first two helices are considered in the context of a larger fragment. The longer peptide, HP−H1/2, includes the first two helices found in HP36 and consists of residues M41−L61. In the native state, 9 of these

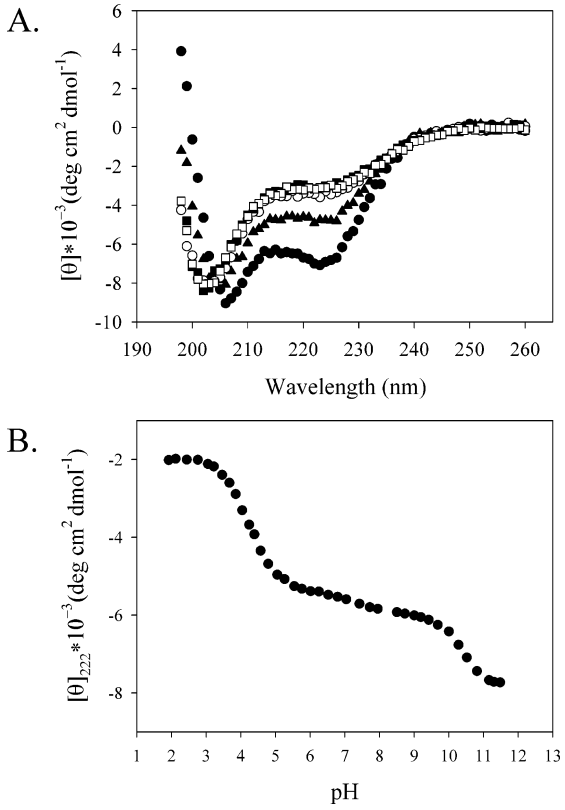

FIGURE 4: Temperature- and pH-dependent CD spectra of HP−H1/2. (A) Temperature-dependent data were collected for a 96.4 μM sample at pH 5.0, 150 mM sodium chloride, and 10 mM sodium acetate. Spectra were recorded at 5 (●), 25 (▲), 45 (○), 60 (■), and 70 °C (□). (B) pH dependence of the CD signal of HP−H1/2 at 222 nm and 25 °C in 150 mM sodium chloride amd 10 mM sodium acetate.

21 residues, or 43%, are helical. This fragment contains the three phenylalanines which contribute to the hydrophobic core. Far-UV CD spectra of a 96.4 μM sample in acetate buffer show that this peptide has significant α-helix content (Figure 4). At pH 5.0 and 25 °C, the mean residue ellipticity at 222 nm is −5000. Decreasing the temperature to 5 °C leads to an increase in signal to −7100 at 222 nm. This corresponds to a nominal helicity of about 20−25%. However, this must be regarded as a crude estimate for several reasons. The first two helices in the native state are quite short, and the CD signal of short helices differs significantly from that of longer helices (*29*). Also, the set of phenylalanines cluster in the native state. Clusters of aromatic residues can affect far-UV CD spectra. The proportion of apparent α-helical structure in HP−H1/2 decreases with increasing temperature. At 45 °C, the value of θ_{222} is reduced by roughly 1/3 compared to the value at 5 °C. Above 45 °C, the spectrum does not change much with temperature. CD spectra were recorded over a range of concentrations varying from 10 to 150 μM to test for any potential self-association. Experiments were conducted at both 5 and 25 °C. The observation that the CD spectrum is independent of concentration from 10 to 150 μM at both temperatures suggests that peptide HP−H1/2 remains monomeric within this concentration range and argues that the structure observed is not due to the association. This was conformed by ultracentrifugation experiments. The results demonstrate that a 350 μM peptide solution remains monomeric at 25 °C (Figure 5). The molecular weight derived

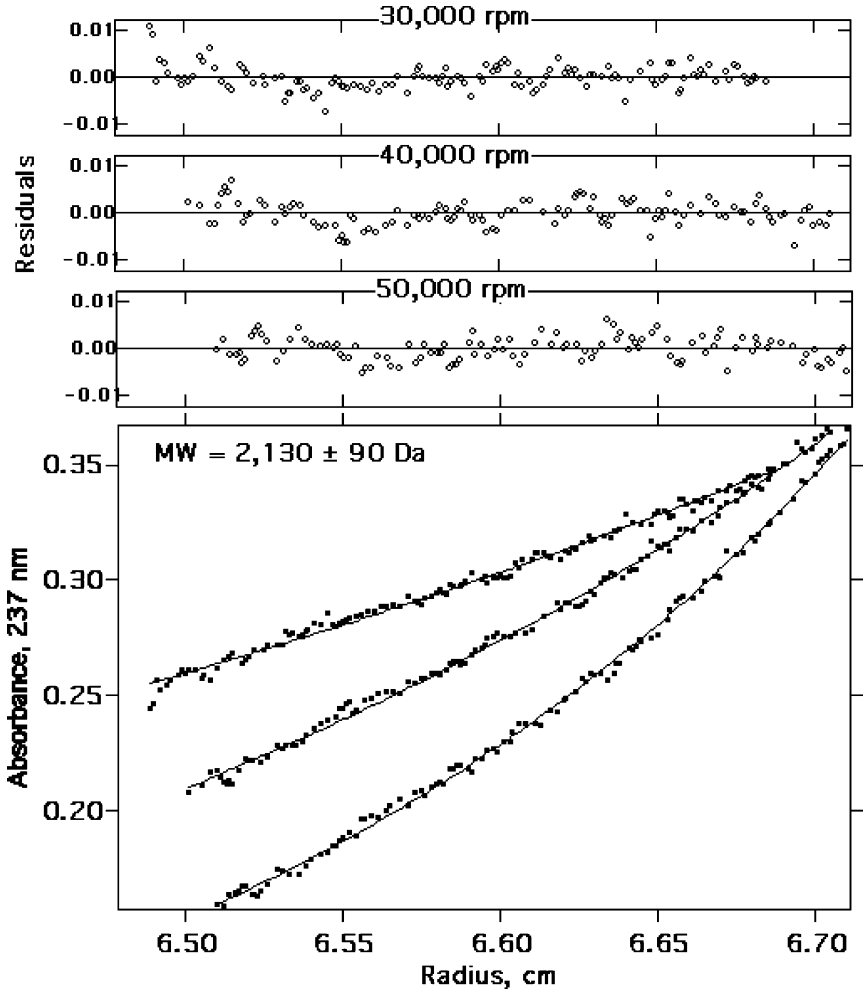

FIGURE 5: Sedimentation equilibrium data for HP−H1/2, collected at three speeds at 25 °C. The molecular weight shown is derived from a simultaneous fitting of data at all three speeds. Samples were prepared at pH 5.0 in 150 mM sodium chloride and 10 mM sodium acetate.

from simultaneously fitting data collected at three speeds is within 5% of the known molecular weight. These studies confirm that the structure detected at 25 °C is not due to association. Centrifugation experiments conducted at 5 °C show that there is some self-association in a 350 μM sample, while a 150 μM sample is predominately (greater than 90%) monomeric. These results indicate that the structures detected by CD at the lower concentrations are not affected by self-association.

A pH titration experiment monitored by CD was performed to determine the dependence of α-helix formation on pH (Figure 4B). The only ionizable groups in this peptide are the N-terminus and several residues in the first helix. The pH dependence of θ_{222} roughly minors that observed for HP−H1. Again, the tendency to form structure is slightly higher at larger pH values due to deprotonation of ionizable residues and/or the free N-terminus, but the effect is fairly modest.

1D NMR spectra in H_2O as well as 2D TOCSY and ROESY spectra in D_2O were collected for a 400 μM sample of HP−H1/2 at pD 5.5. 1D spectra in D_2O were also recorded at 150 and 400 μM. Two interesting features are present in the 1D NMR spectrum: a strongly upfield-shifted resonance at 0.32 ppm (Figure 6C) and a set of upfield-shifted Phe resonances (Figure 7B). The resonances are not due to structure induced by association since they are present in both the 150 and 400 μM samples. The peaks are broader in the 400 μM sample, but the chemical shifts are not changed. In wild-type HP36, the most upfield-shifted resonance is at −0.11 ppm, and it is due to one of the methyl groups of Val 50. For comparison, the random coil chemical shifts of valine methyls are between 0.93 and 0.96 ppm (*24*). A TOCSY spectrum recorded in D_2O indicates that the strongly upfield-shifted resonance in HP−H1/2 is from the methyl group of the only Val (Val 50). Val 50 is also present in HP−H1 and HP−H4, and both of these peptides contain two of the three phenylalanines. However, the Val 50 resonance is not shifted away from random coil values (Figure 6A,B) in the shorter peptides. This is an interesting observation since it indicates that the features that induce this large shift are not due to short-range local effects but require more of the peptide chain. The large upfield shift must be due to interactions with one or more of the phenylalanine rings. To confirm this, a 1D NOE difference experiment was performed at 25 °C by saturating the methyl peak. NOEs were observed to resonances at 4.23, 2.18, and 0.89 ppm which correspond to the α proton, the β proton, and the other methyl of Val 50. Resonances in the aromatic region also show a negative NOE enhancement, confirming that the methyl group is close to one or more aromatic rings. Temperature-dependent 1D NMR experiments show that the Val 50 resonance shifts farther upfield as the temperature is lowered. The peak is shifted to 0.11 ppm at 13.6 °C. The Val 50 methyl resonance is broader than the other peaks, which may reflect a

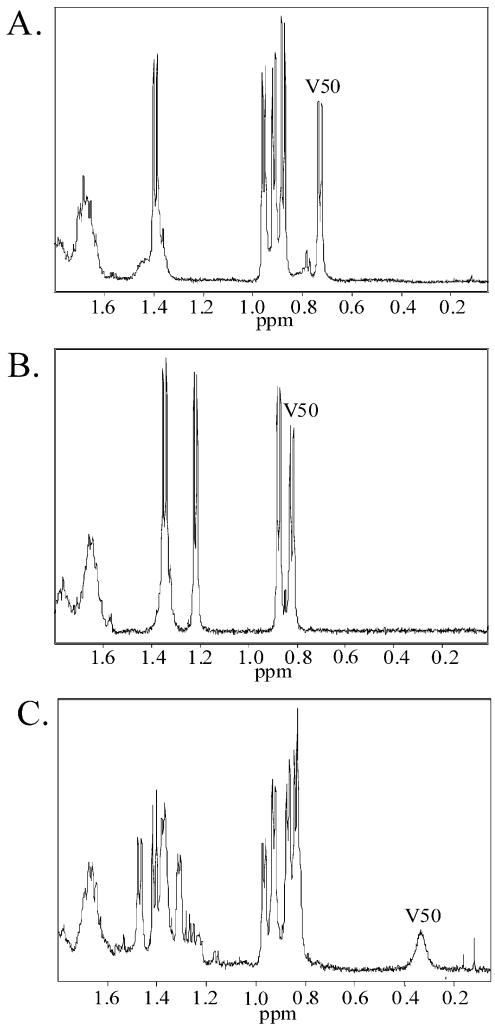

FIGURE 6: Upfield region of the one-dimensional proton NMR spectra of (A) HP−H1, (B) HP−H4, and (C) HP−H1/2. Spectra were acquired at 25 °C in 150 mM sodium chloride and 10 mM sodium acetate buffer at pH 5.5 for HP−H1 and pH 5.0 for HP−H1/2. The methyl resonance of V50 is labeled.

contribution from exchange broadening. Changes are also observed in the aromatic region, with several phenylalanine resonances shifting upfield as the temperature is decreased. There are several strongly upfield-shifted phenylalanine ring resonances in the native state of intact HP36. The upfield region and aromatic region of HP−H1/2, recorded at 13.6 and 74.5 °C, respectively, are compared in Figure 7. The data clearly show that the tertiary interactions observed at low temperature are absent or are significantly reduced at high temperatures.

Temperature-dependent ^{1}H NMR studies provide evidence for similar structure in the thermally denatured state of intact HP36. We have previously estimated the folding rate of HP36 using dynamic NMR line shape analysis (*7*). In these experiments, exchange-broadened resonances are simulated to obtain the exchange rate. The fitting procedure also provides an estimation of the denatured state chemical shift at a given temperature (*30*, *31*). Thus, the chemical shift of the Val 50 resonance in HP−H1/2 can be compared to the estimated chemical shift of this resonance in the denatured state of the intact protein (Figure 8). The results of the line shape simulations indicate that there is structure in the denatured state of HP36 which shifts the methyl resonance

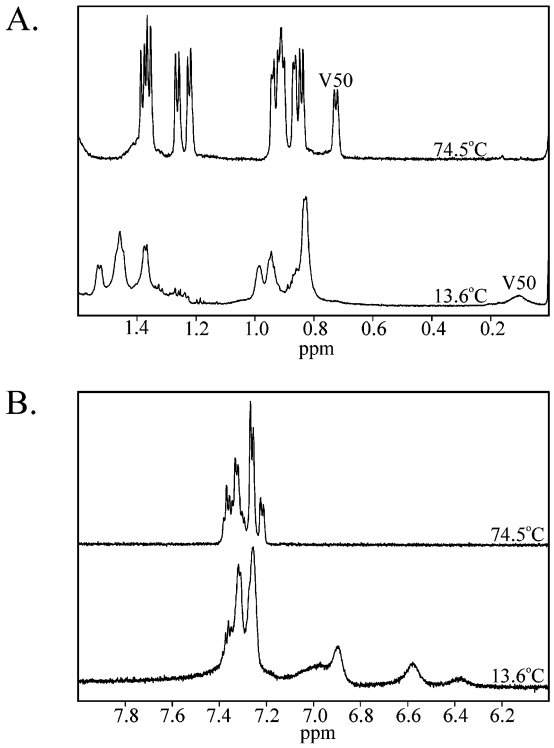

FIGURE 7: One-dimensional proton NMR spectra of HP−H1/2 at high and low temperatures: (A) unfield region and (B) aromatic region. Spectra were recorded at 13.6 and 74.5 °C at pD 5.5 (uncorrected) in 150 mM sodium chloride and 10 mM sodium acetate in D_2O buffer.

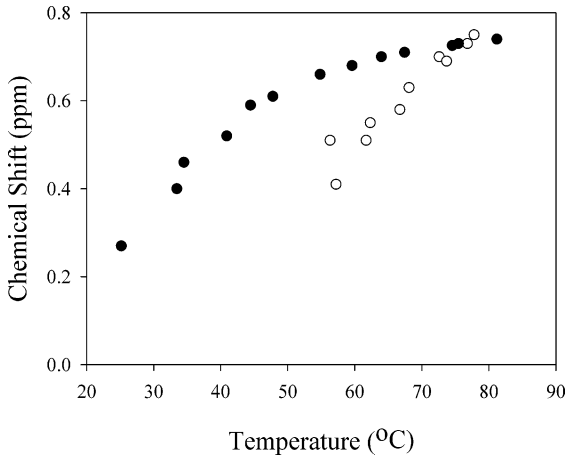

FIGURE 8: Denatured state chemical shifts for the upfield Val 50 methyl resonance of intact HP36 estimated by line shape simulation as described in the text (○), and measured chemical shifts of Val 50 in HP−H1/2 (●). For reference, the random coil chemical shifts of valine methyls are between 0.93 and 0.96 ppm at 25 °C (*24*).

of Val 50. The measured chemical shift of the resonance in HP−H1/2 is always closer to random coil than is the calculated denatured state shift for intact HP36. The analysis highlights two important points. First, the observation of the strongly ring-current-shifted resonance in both systems suggests that similar structure is likely present. Second, the fact that the resonance in thermally unfolded HP36 is more strongly shifted argues that the structure is more developed in the intact molecule, i.e., that the rest of the chain helps to stabilize the denatured state structure.

Aromatic Residues Play a Critical Role in Stabilizing the Structure. The native state of HP36 contains a cluster of three

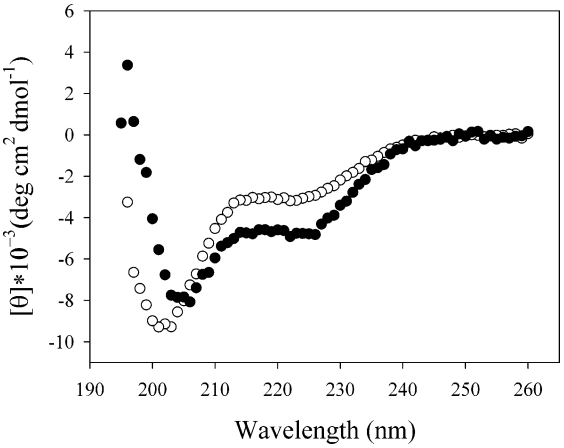

FIGURE 9: Far-UV CD spectra for F47L,F51L,HP−H1/2 (○) and HP−H1/2 (●) recorded at pH 5.0 and 25 °C in 150 mM sodium chloride and 10 mM sodium acetate.

phenylalanine residues which make a significant contribution to the hydrophobic core. Mutation of these residues has been shown to affect the stability of HP36. McKnight and coworkers have shown that simultaneous mutation of Phe 47 and Phe 51 to leucine results in a protein which is significantly less stable but which still folds to the same native structure (*26*). Simultaneous mutation of any other combination of two of the buried phenylalanines results in proteins which do not fold. Consequently, we prepared an analogue of HP−H1/2 in which Phe 47 and Phe 51 were replaced by leucine. The construct is designated F47L,F51L, HP−H1/2. The results of these substitutions are dramatic. The peptide is considerably less structured than HP−H1/2. The CD spectra of the two peptides are compared in Figure 9, and the spectrum of HP−H1/2 clearly indicates significant loss of structure. The value of θ_{222} at 25 °C is reduced by almost 50%, to −3100, for the mutant peptide. One-dimensional NMR experiments support the CD measurements and indicate that the peptide is much less structured. No ring-current-shifted resonances are observed, and both the methyl and aromatic resonances are clustered near random coil values.

DISCUSSION

These experiments strongly suggest that there is significant structure in the denatured state of HP36 which is not due simply to locally stabilized structure. The studies of the HP−H1, HP−H2, HP−H3, and HP−H4 set of peptides show that there is no significant tendency for any element of secondary structure to fold in isolation. Analysis of the HP−H1/2 peptide indicates that longer range contacts are required. This work shows that, compared to HP−H1 or HP−H4, the region near Val 50 becomes structured in the larger HP−H1/2 peptide. The fact that HP−H4 is unstructured argues that the increased structure observed in HP−H1/2 compared to HP−H1 is not simply because the position of the C-terminus has moved in HP−H1/2 relative to HP−H1. Analysis of the observed chemical shifts and 1D NOE data clearly demonstrates that interactions involving Val 50 and one or more aromatic residues play a role. Analysis of the peptide in which Phe 47 and Phe 51 are replaced by leucine confirms that aromatic residues play an important role in stabilizing this structure. In addition, the pH-dependent studies suggest that interactions involving ionized acidic residues also play a role in stabilizing the structure. It must be stressed that it is not possible to determine if the structure is native-like or involves non-native interactions. The observation of a significant shift for the Val 50 methyl is consistent with native-like interactions but of course does not provide direct proof. It is also worth noting that six of the seven most protected amides observed in the native state exchange experiments are located in this region (*4*). All of these have free energies of opening which are at least 1 kcal mol^{-1} greater than the global free energy of unfolding. Interestingly, only one of these six amides is located within one of the helical regions. This highlights the conclusions obtained with our peptide studies, namely that the denatured state structure is not due simply to unusually stable helices. HP36 is one of the fastest folding proteins known and has become an extremely popular system for computational and theoretical studies of protein folding (*9*−*21*). Thus, the observation of significant structure in its denatured state is of particular interest.

ACKNOWLEDGMENT

We thank Francis Picart for assistance with some of the NMR measurements. We thank Professor Simmerling, Ms. Lauren Wickstrom, and Mr. Picart for helpful discussions. We thank Professor Jamie McKnight for numerous helpful discussions and for his continued interested in these studies.

SUPPORTING INFORMATION AVAILABLE

Table of ^{1}H chemical shifts for HP−H1, HP−H2, HP−H3 and HP−H4; pH dependence of the CD signal for HP−H1 and HP−H3; 1D difference NOE ^{1}H NMR spectrum of HP−H1/2; and a portion of the TOCSY spectrum of HP−H1/2. This material is available free of charge via the Internet at http://pubs.acs.org.

REFERENCES

1. Shortle, D. (1996) *FASEB J. 10*, 27−34.
2. Dill, K. A., and Shortle, D. (1991) *Annu. Rev. Biochem. 60*, 795−825.
3. Wright, P. E., Dyson, H. J., and Lerner, R. A. (1988) *Biochemistry 27*, 7167−7175.
4. McKnight, C. J., Doering, D. S., Matsudaira, P. T., and Kim, P. S. (1996) *J. Mol. Biol. 260*, 126−134.
5. McKnight, C. J., Matsudaira, P. T., and Kim, P. S. (1997) *Nat. Struct. Biol. 4*, 180−184.
6. Vardar, D., Buckley, D. A., Frank, B. S., and McKnight, C. J. (1999) *J. Mol. Biol. 294*, 1299−1310.
7. Wang, M., Tang, Y., Sato, S., Vugmeyster, L., McKnight, C. J., and Raleigh, D. P. (2003) *J. Am. Chem. Soc. 125*, 6032−6033.
8. Kubelka, J., Eaton, W. A., and Hofrichter, J. (2003) *J. Mol. Biol. 329*, 625−630.
9. Islam, S. A., Karplus, M., and Weaver, D. L. (2002) *J. Mol. Biol. 318*, 199−215.
10. Duan, Y., and Kollman, P. A. (1998) *Science 282*, 740−744.
11. Duan, Y., Wang, L., and Kollman, P. A. (1998) *Proc. Natl. Acad. Sci. U.S.A. 95*, 9897−9902.
12. Sullivan, D. C., and Kuntz, I. D. (2002) *J. Phys. Chem. B 106*, 3255−3262.
13. Shen, M. Y., and Freed, K. F. (2002) *Proteins 49*, 439−445.
14. Srinivas, G., and Bagchi, B. (2002) *Curr. Sci. 82*, 179−185.
15. Fernandez, A., Shen, M. Y., Colubri, A., Sosnick, T. R., Berry, R. S., and Freed, K. F. (2003) *Biochemistry 42*, 664−471.
16. Zagrovic, B., Snow, C. D., Shirts, M. R., and Pande, V. S. (2002) *J. Mol. Biol. 323*, 927−937.
17. Zagrovic, B., Snow, C., Khaliq, S., Shirts, M., and Pande, V. (2002) *J. Mol. Biol. 323*, 153−164.

18. Lin, C. Y., Hu, C. K., and Hansmann, U. H. (2003) *Proteins 52*, 436−445.
19. He, J. B., Zhang, Z. Y., Shi, Y. Y., and Liu, H. Y. (2003) *J. Chem. Phys. 119*, 4005−4017.
20. Jang, S. M., Kim, E., Shin, S. and Pak, Y. (2003) *J. Am. Chem. Soc. 125*, 14841−14846.
21. van der Spoel, D., and Lindahl, E. (2003) *J. Phys. Chem. B 107*, 11178−11187.
22. Karplus, M., and Weaver, D. L. (1976) *Nature 260*, 404−406.
23. Pace, C. N., Vajdos, F., Fee, L., Grimsley, G., and Gray, T. (1995) *Protein. Sci. 4*, 2411−2423.
24. Wishart, D. S., Bigam, C. G., Holm, A., Hodges, R. S., and Sykes, B. D. (1995) *J. Biomol. NMR 5*, 67−81.
25. Laue, T., Shaw, B. D., Ridgeway, T. M., and Pelletier, S. L. (1992) in *Analytical Ultracentrifugation in Biochemistry and Polymer Science* (Harding, S. E., Rowe, A., and Horton, J. C., Eds.) pp 90−125, The Royal Society of Chemistry, Cambridge, UK.
26. Frank, B. S., Vardar, D., Buckley, D. A., and McKnight, C. J. (2002) *Protein. Sci. 11*, 680−687.
27. Rohl, C. A., and Baldwin, R. L. (1997) *Biochemistry 36*, 8435−8442.
28. Smith, L. J., Fiebig, K. M., Schwalbe, H., and Dobson, C. M. (1996) *Fold. Des. 1*, R95−106.
29. Woody, R. W. (1996) in *Circular dichroism and the conformational analysis of biomolecules* (Fasman, G. D., Ed.) pp 25−67, Plenum Press, New York.
30. Huang, G. S., and Oas, T. G. (1995) *Proc. Natl. Acad. Sci. U.S.A. 92*, 6878−6882.
31. Kuhlman, B., Boice, J. A., Fairman, R., and Raleigh, D. P. (1998) *Biochemistry 37*, 1025−1032.
32. Kraulis, P. J. (1991) *J. Appl. Crystallogr. 24*, 946−950.

BI035652P